

Ignition Characteristics of Methane and Hydrogen Using a Plasma Torch in Supersonic Flow

Tomoaki Kitagawa,* Atsushi Moriwaki,[†] Koichi Murakami,[‡] Kenichi Takita,[§] and Goro Masuya[¶]
Tohoku University, Sendai 980-8579, Japan

Ignition and flame-holding characteristics of methane and hydrogen using a plasma torch igniter were experimentally investigated in a supersonic airflow. The main airflow Mach number was 2.3, and the stagnation pressure and temperature corresponded to atmospheric conditions. Nitrogen, oxygen, a hydrogen/nitrogen mixture, and a methane/nitrogen mixture were used as feedstocks for the torch. The fuel was vertically injected from the wall where the plasma torch was attached. The wall pressure and the total temperature at the exit of the test section were measured. Ignition was confirmed for hydrogen injected both upstream and downstream of the torch. No strong dependence on the kind of feedstock of the torch for effectiveness of ignition of the hydrogen fuel was evident in a supersonic flow. By contrast, ignition of the methane fuel was confirmed only when it was injected upstream of the torch. In addition, the wall-pressure increase of the methane fuel was about half that of the hydrogen fuel. An important result for methane fuel was that using oxygen as a feedstock resulted in the most remarkable increase of the total temperature and the wall pressure.

Nomenclature

C	=	mole fraction
M	=	Mach number
m	=	mass flow rate
P	=	electric power input
p	=	pressure
ΔT	=	temperature increase
x, y	=	Cartesian coordinates

Subscripts

av	=	average
CH ₄	=	methane
comb	=	combustion, fuel + plasma jet
H ₂	=	hydrogen
IN	=	input
i	=	injector
O	=	oxygen atom
PJ	=	plasma torch
t	=	stagnation condition
0	=	undisturbed airstream

Introduction

ONE of the most important technologies for the scramjet engine is reliable ignition of the fuel. The plasma jet (PJ) torch has many attractive advantages that make it suitable for use as the igniter of the scramjet engine.^{1–7} For example, it continuously provides high-temperature gas containing various radical species, which is generated by arc discharges and can be changed by variation of feedstocks; most feedstocks are thermally stable and neither toxic nor

corrosive. Thus, the ignition characteristics of fuels with a plasma torch in high-speed flow are important for the development of the scramjet engine.

Hydrocarbon fuels are candidates for use in the scramjet engine.^{8,9} They have many operational advantages for application to hypersonic flight systems in comparison with hydrogen (H₂): for example, high density, low production cost, and storability. In particular, low fuel-tank volume due to the high density of hydrocarbon fuels results in reductions of the dry mass and aerodynamic drag and increase of the payload. Considering the total system of the vehicle, these advantages of hydrocarbon fuels are important. Methane (CH₄) is more promising for flight up to low hypersonic speed compared with other hydrocarbon fuels because it has the highest specific impulse and cooling capability.^{10–12} However, hydrocarbon fuels are more difficult to ignite than hydrogen. Methane has a longer ignition delay time than hydrogen,^{11,13} but it is possible to enhance ignition and combustion of CH₄ via the effect of radicals supplied by the plasma torch with suitably selected feedstock. Therefore, understanding the ignition characteristics of CH₄ fuel in the PJ is important. The purpose of the present study was to experimentally investigate and understand the ignition characteristics of CH₄ in the PJ, including the effect of the combination of feedstock and fuel, and to compare the characteristics with those of H₂.

Experimental Apparatus

Wind Tunnel and Test Section

The experiment was conducted using an intermittent suction-type wind tunnel shown in Fig. 1. When a butterfly valve between the test section and the evacuated tank was opened, atmospheric air was inhaled and accelerated to supersonic speed through a two-dimensional contoured nozzle. Figure 2 shows a schematic of the test section. The test section had a 30-mm square uniform cross section and was 335 mm long. The sidewalls of the test section were made of quartz glass for observation of the flowfield and combustion conditions. The main flow Mach number calculated from the wall pressure in the test section with the isentropic relation was 2.3. The mass flow rate was 73.4 g/s for the stagnation condition of 273.15 K and 100 kPa, and the unit Reynolds number was $1.1 \times 10^7 \text{ m}^{-1}$.

The plasma torch was placed on the centerline of the bottom wall of the test section 215 mm downstream from the entrance of the test section. The origin of the Cartesian coordinate system was considered to be at the center of the torch nozzle exit. The x axis was in the streamwise direction, and the y axis was in the injection direction.

Presented as Paper 2002-5210 at the AIAA/AAAF 11th Space Planes and Hypersonic Systems and Technologies, Orleans, France, 29 September–4 October 2002; received 16 January 2003; revision received 28 April 2003; accepted for publication 11 May 2003. Copyright © 2003 by the American Institute of Aeronautics and Astronautics, Inc. All rights reserved. Copies of this paper may be made for personal or internal use, on condition that the copier pay the \$10.00 per-copy fee to the Copyright Clearance Center, Inc., 222 Rosewood Drive, Danvers, MA 01923; include the code 0748-4658/03 \$10.00 in correspondence with the CCC.

*Graduate Student, Department of Aeronautics and Space Engineering.

[†]Graduate Student, Department of Aeronautics and Space Engineering.

[‡]Graduate Student, Department of Aeronautics and Space Engineering.

[§]Associate Professor, Department of Aeronautics and Space Engineering; takita@cc.mech.tohoku.ac.jp. Member AIAA.

[¶]Professor, Department of Aeronautics and Space Engineering. Senior Member AIAA.

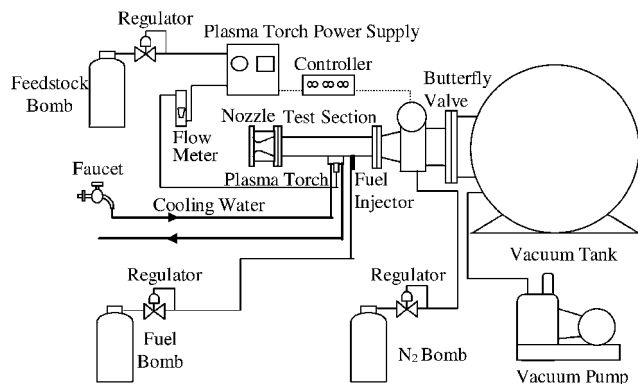


Fig. 1 Schematic diagram of experimental apparatus.

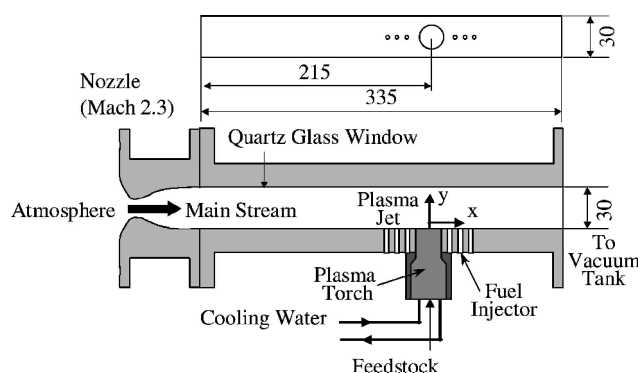


Fig. 2 Schematic diagram of nozzle and test section (dimensions in millimeters).

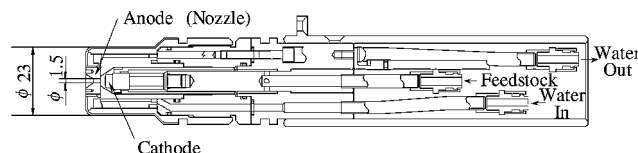


Fig. 3 Schematic of plasma torch (dimensions in millimeters).

Plasma Torch

The plasma torch configuration is shown in Fig. 3. The cathode was made of hafnium to attain high durability when oxygen was used as the feedstock. The anode and the nozzle were made of oxygen-free copper. The diameter of the torch nozzle throat was 1.5 mm. The PJ was injected normal to the main stream. The torch was water-cooled to allow high electric power input. The plasma torch feedstock used for the methane fuel was oxygen, nitrogen, a hydrogen/nitrogen mixture (hydrogen mole fraction of 0.30), or a methane/nitrogen mixture (methane mole fraction of 0.10). For the hydrogen fuel, the feedstock was oxygen, nitrogen, or hydrogen/nitrogen (hydrogen mole fraction of 0.30). The total mole flow rate of the feedstocks was set at 1.1×10^{-2} mol/s for all cases. The direct current power unit supplied electric power input to the torch from 1.5 to 3.5 kW. For the oxygen feedstock, the electric power input was limited to less than 2.5 kW to suppress damage to the electrodes and to maintain stable operation.

Fuel Injector

The fuel-injection orifice was placed at the center of the bottom wall at $x_i = -34, -26, -18, 18, 26,$ or 34 mm. The diameter of the orifices was 1.0 mm. The fuel was gaseous methane or hydrogen at room temperature. The fuel was injected normal to the main stream at sonic speed from one of the fuel-injection orifices. The dynamic pressure ratio of the fuel jet and the main flow was set at 3 in all cases. The mass flow rate of the methane fuel was 0.35 g/s and the rate of the hydrogen fuel was 0.12 g/s for the stagnation condition

of 273.15 K and 100 kPa. The total equivalence ratio was 0.081 for methane and 0.057 for hydrogen. Such low values of equivalence ratio were required to avoid thermal choking of the flow, because the air was not heated.

Measurement

The flow was visualized via schlieren method using a stroboscope lamp with a pulse time of 70 ns. The wall pressure on the centerline of the bottom wall of the test section was measured by a strain-gauge-type pressure transducer attached to a mechanical pressure scanner through pressure taps 1.0 mm in diameter. The flow rate of the feedstock was measured by a float-type flowmeter. The dynamic pressure ratio of the fuel jet and the main flow was adjusted by measuring the stagnation pressure of the fuel with a strain-gauge-type pressure transducer. The total temperature at the exit of the test section was measured by a ten-point stagnation temperature probe rake with K-type thermocouples vertically attached to the center of the exit of the test section (120 mm downstream of the PJ). The outer diameter of each temperature probe was 1.9 mm, and each probe had two small vent holes on the sidewall. The recovery factor of the probes was 0.98. The total cross-sectional area of the temperature probes was 3.2% of the exit area of the test section. The temperature was measured 6 s after the plasma torch was started. When ignition occurred, remarkable increases of the wall pressure and the total temperature were observed.

Results

Definition of Success in Ignition and Flame-Holding

Typical examples of measured temperature and wall pressure for cases of both ignition and nonignition are presented in this section. The establishment of ignition and flame-holding is discussed based on these data. Large increases in the wall pressure and temperature were due to heat release by combustion in the large area after local ignition. In other words, flame-holding was never attained without ignition. Therefore, ignition and flame-holding were not distinctly separated in many cases.

Figure 4 shows distribution of temperature increase from the freestream condition at the exit of the test section for fuel (CH_4) injected at $x_i = 18$ mm. The feedstock and the electric power input were nitrogen and 2.3 kW, respectively. When the fuel was injected without the PJ, the temperature decreased near the bottom wall, confirming that the fuel was distributed below $y = 10$ mm at the exit. When the PJ was operated without fuel injection, the temperature increased throughout the exit section; namely, it was about 100 K higher than the freestream temperature near the bottom wall.

For the case of PJ operation with CH_4 injection, the temperature close to the bottom wall decreased from the level for the case with only PJ due to the cool fuel. However, an increase of temperature in the case of PJ with CH_4 injection was observed in the medium-height region, suggesting that heat release by reaction locally occurred. For the case of the PJ with H_2 injection, there was a large temperature increase at all heights that were about twice that for the case of only

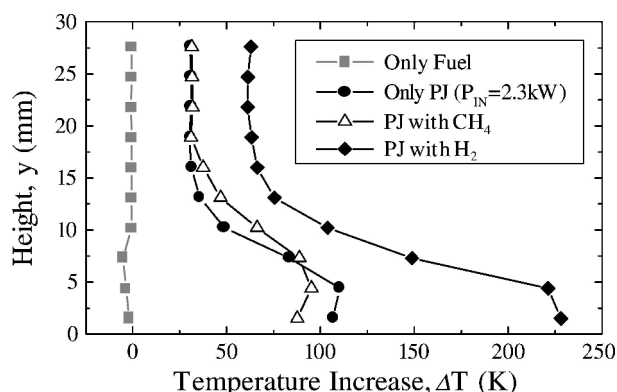


Fig. 4 Distributions of temperature increase at exit of test section ($x_i = 18$ mm, N_2 PJ, $P_{\text{IN}} = 2.3$ kW).

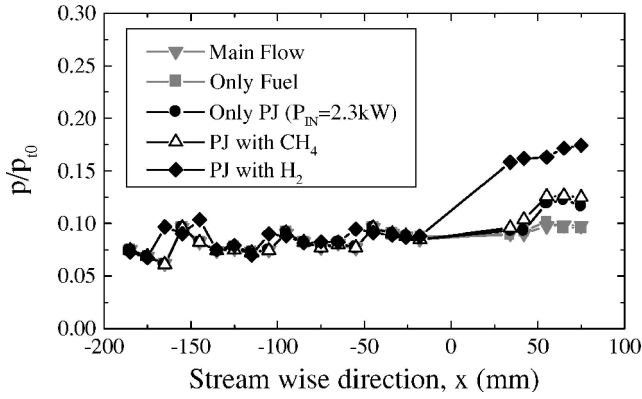


Fig. 5 Distributions of wall pressure ($x_i = 18$ mm, N_2 PJ, $P_{IN} = 2.3$ kW).

PJ. The H_2 burned very well in this condition. The maximum temperature increase was obtained near the bottom wall and, therefore, it was concluded that combustion occurred mainly near the wall around the PJ plume.

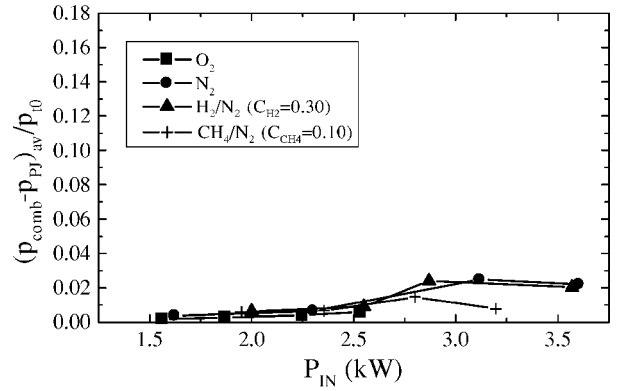
Figure 5 shows wall-pressure distributions corresponding to the cases shown in Fig. 4. The wall pressure was normalized by the freestream stagnation pressure. The magnitude of error bars was within 10% throughout the experiments except in regions where the pressure suddenly changed. For the case of fuel only, the wall-pressure distribution was the same as that for the main flow without any disturbance. Though the fuel injection without PJ operation caused a slight decrease of temperature at the exit section, it had almost no effect on the freestream condition. In the case of PJ only, a pressure rise was observed downstream of the PJ caused by the high-temperature PJ plume. There was little difference in the wall-pressure distributions between the case of PJ only and that of PJ with CH_4 . This indicates that no significant combustion of the CH_4 fuel occurred around the PJ in this configuration, although reaction might have occurred locally in a small region. For the case of PJ with H_2 , however, a large pressure increase was obtained by ignition and stable combustion of the H_2 fuel in a large area.

The behavior of the wall pressure corresponded well with that of the temperature distribution at the exit of the test section. Therefore, success of ignition and flame-holding of the fuel using the PJ could be judged by consideration of data for both.

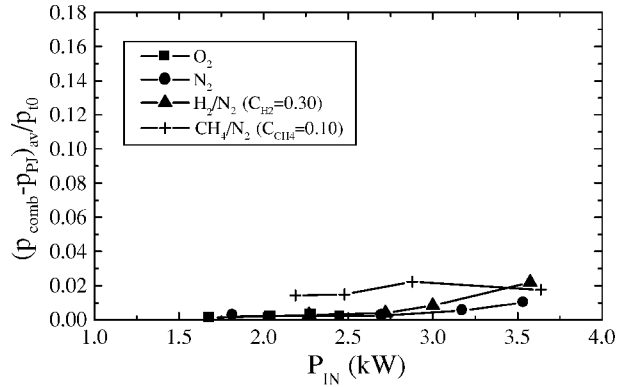
Fuel Injection Downstream of PJ

Figures 6a and 6b show nondimensional averaged pressure increases, $(p_{comb} - p_{PJ})_{av} / p_{10}$, plotted for P_{IN} for the CH_4 fuel injected downstream of the PJ at $x_i = 18$ and 34 mm, respectively. Four feedstock gases (O_2 , N_2 , H_2/N_2 , and CH_4/N_2) were tested. The averaged values were calculated by taking the algebraic mean of the data for all the pressure taps downstream of the PJ. In the case of the CH_4 fuel, the pressure increase was very small for all feedstocks and for both injection locations. The distribution of the temperature at the exit also showed a very small increase (about 20 K). Slight increases for large P_{IN} were caused by local combustion around the high-temperature plume of the PJ. The degree of local combustion was slightly greater for $x_i = 18$ mm because the PJ plume had a higher temperature at the point of fuel injection. The CH_4/N_2 PJ⁹ which included CH_4 fuel as a component of the feedstock, was newly tested for ignition of the CH_4 main fuel. However, no superiority to other PJs was apparent. Slight increase in the wall pressure for the CH_4/N_2 PJ in Fig. 6b was a result of combustion of CH_4 included in the feedstock after injection in the airflow, because such a slight increase was also obtained for PJ-only injection.

Figures 7a and 7b show the averaged pressure increases by combustion of the H_2 fuel injected downstream of the PJ. Pressure increases for the H_2 fuel were much larger than those for the CH_4 fuel, as shown in Figs. 6. The existence of threshold values of P_{IN} achieving strong combustion was shown as reported in Ref. 5. It can be concluded from Figs. 7 that the H_2/N_2 PJ was the most efficient

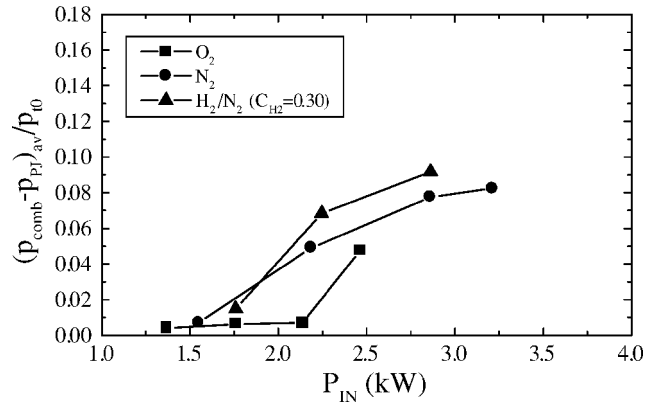


a) $x_i = 18$ mm

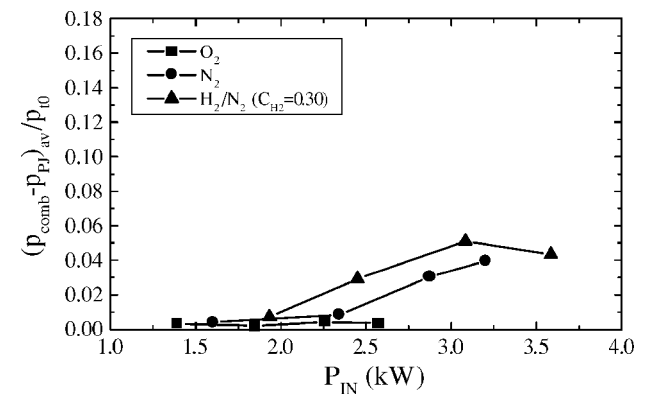


b) $x_i = 34$ mm

Fig. 6 Average pressure increase at wall by combustion of CH_4 fuel injected downstream of PJ.



a) $x_i = 18$ mm



b) $x_i = 34$ mm

Fig. 7 Average pressure increase at wall by combustion of H_2 fuel injected downstream of PJ.

for ignition and combustion of H_2 fuel in a supersonic airflow and that the O_2 PJ was the worst. The order of effectiveness among the PJs was the same as that obtained in the previous experiments in a subsonic flow.¹³ The superiority of the H_2/N_2 PJ to the others, however, was much more remarkable in the case of subsonic flow.¹³ The reason for this difference is thought to be a low diffusivity of the PJ plume in a supersonic flow. The contribution of reaction of nondissociated H_2 molecules of the H_2/N_2 PJ injected into a supersonic airflow must be less than that injected into a subsonic stream.

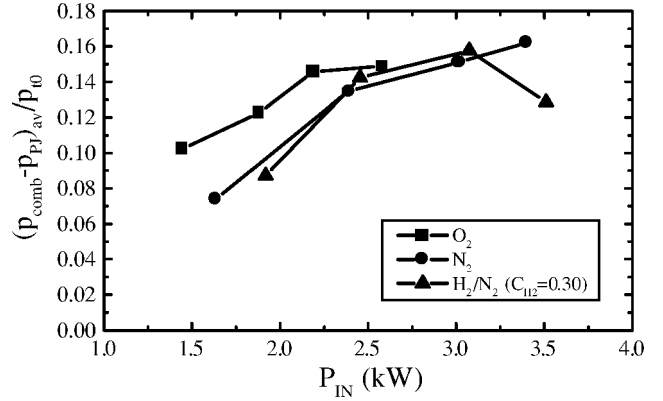
In the case of fuel injection downstream of the PJ, the temperature of the PJ plume at the point of fuel injection was considered to be an important factor for ignition and combustion of the fuel. The H_2/N_2 PJ had the highest temperature at the exit of the duct when only the PJ was injected, whereas the O_2 PJ had the lowest. When the distance between the PJ and the fuel jet was decreased, ignition and combustion easily occurred at low P_{IN} and the pressure increase became large. The reason for this was considered to be a rapid decrease in the temperature of the PJ plume.

Fuel Injection Upstream of PJ

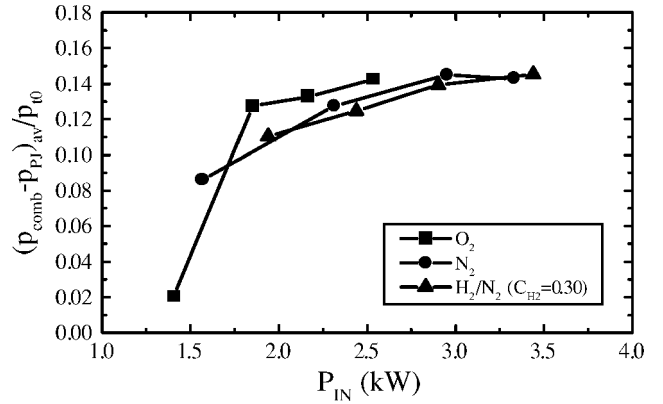
Figures 8a and 8b show averaged pressure increases by the CH_4 jet injected upstream of the PJ at $x_i = -18$ and -34 mm, respectively. In the case of fuel injection upstream of the PJ, ignition and combustion easily occurred and the pressure increase was roughly in proportion to P_{IN} . The temperature distribution at the exit also showed a large increase due to strong combustion.

In Fig. 8, the superiority of the O_2 PJ to other PJs was remarkable. Strong combustion occurred even for the lowest P_{IN} (about 1.3 kW) supplied by the power unit used in the present experiment. On the other hand, other PJs showed only a slight difference from one another. Such superiority of the O_2 PJ for ignition and flame-holding of the CH_4 fuel was also observed in the experiment performed by Shuzenji and Tachibana.¹²

When the distance between the PJ and the fuel jet was large, the pressure increase became large and the minimum P_{IN} required for



a) $x_i = -18$ mm



b) $x_i = -34$ mm

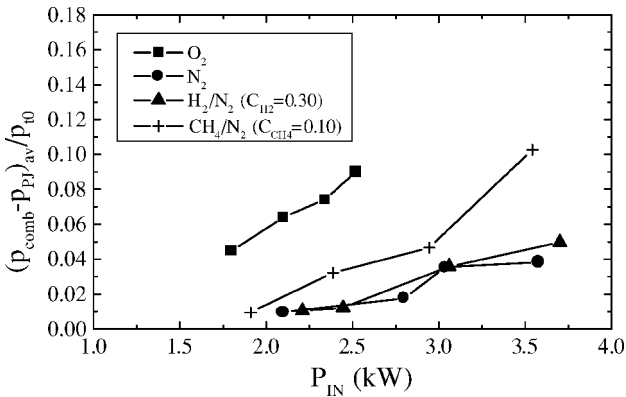
Fig. 9 Average pressure increase at wall by combustion of H_2 fuel injected upstream of PJ.

ignition became small. This result suggested that the local equivalence ratio at the PJ torch nozzle was important for determination of the amount of combustion and of which mixture was most suitable. CH_4 requires a greater amount of air for combustion compared with H_2 , so the effect of premixing by diffusion became greater.

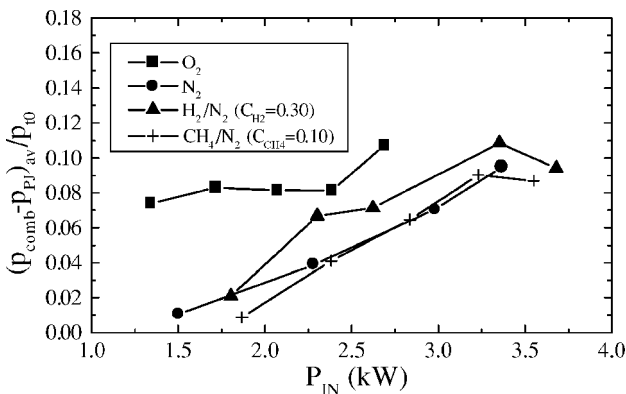
Figures 9a and 9b show averaged pressure increases by the H_2 jet injected upstream of the PJ. Strong combustion of the H_2 fuel easily occurred even at low P_{IN} . Although the total equivalence ratio of the H_2 fuel was smaller than that of the CH_4 fuel, the degree of pressure increase by combustion was greater than that of the CH_4 fuel and it maintained a constant value for high P_{IN} .

The aforementioned results, showing the superiority of the injection upstream of the PJ in ignition to the downstream injection for both fuels, were in good agreement with findings of other experiments⁵ and numerical simulations.⁶ In the case of upstream injection, the PJ was considered to become a flame-holder itself as well as an igniter.

Figure 10 shows the schlieren and direct photographs for the CH_4 fuel injected at $x_i = -34$ mm. The electric power input was 2.0 kW and the feedstock was N_2 (Figs. 10a, 10c, 10e and 10g) or O_2 (Figs. 10b, 10d, 10f and 10h). For the cases of PJ-only injection, there was no difference between the effects of N_2 and O_2 feedstocks on the penetration height of the PJ or PJ plume. For the CH_4 fuel injection, however, there was a very large difference between the two feedstocks. The direct photograph shows that the N_2 PJ resulted in a burning region that was much more luminous than that with the O_2 PJ. In the schlieren photograph, however, the shock wave formed from heat release of combustion by the O_2 PJ can be seen to be stronger than that in the case of the N_2 PJ. It is known that such shock waves drastically enhance the mixing and combustion downstream.¹⁴ In Fig. 8, the injection of the O_2 PJ even at the lowest electric power input resulted in a large pressure increase; this was considered to be a cause of such shock waves.



a) $x_i = -18$ mm



b) $x_i = -34$ mm

Fig. 8 Average pressure increase at wall by combustion of CH_4 fuel injected upstream of PJ.

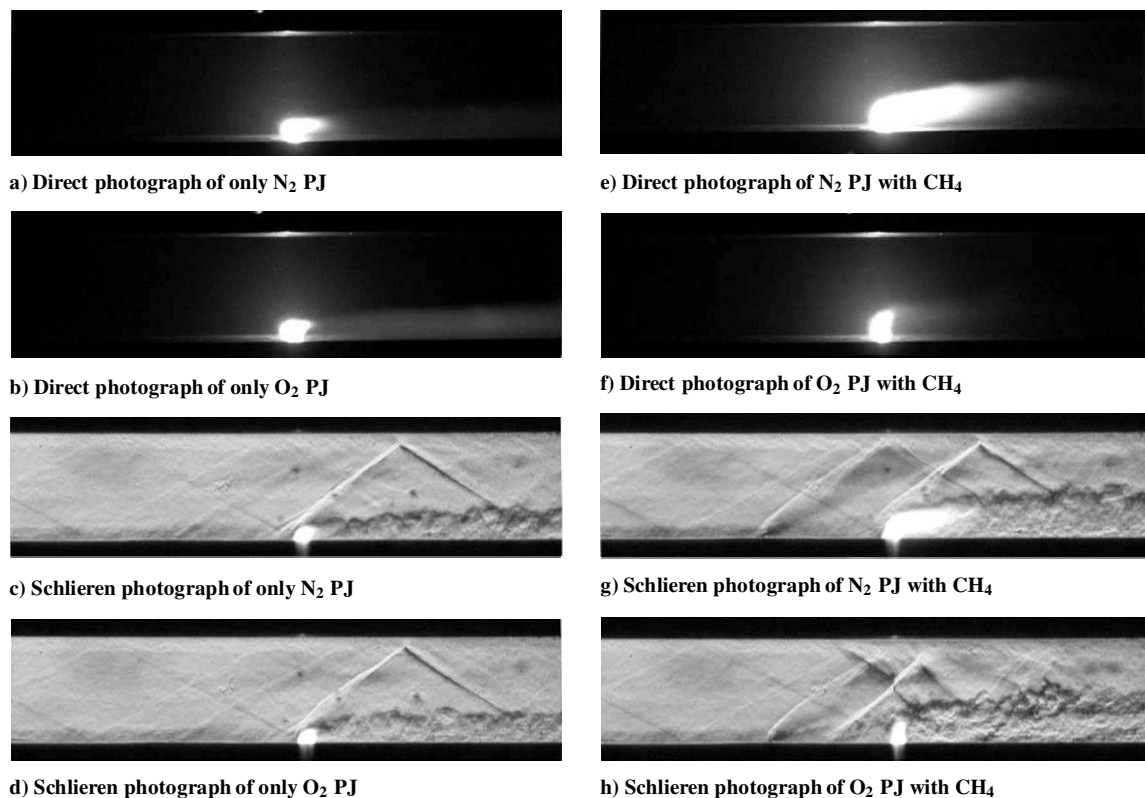


Fig. 10 Schlieren and direct photographs ($x_i = -34$ mm, N₂ or O₂ PJ, $P_{IN} = 2.0$ kW).

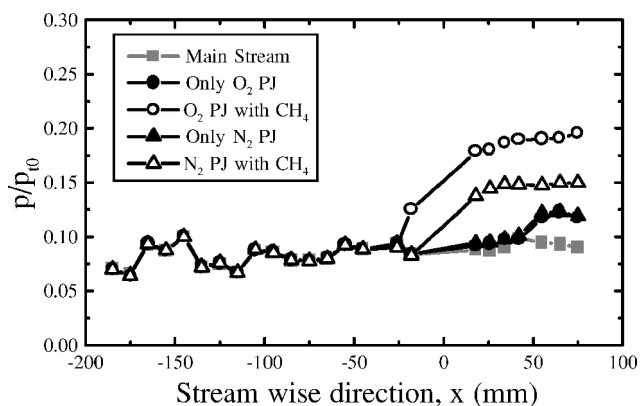


Fig. 11 Distributions of wall pressure ($x_i = -34$ mm, N₂ or O₂PJ, $P_{IN} = 2.0$ kW).

The wall-pressure rise corresponding to the case in Fig. 10 is shown in Fig. 11. Both cases of only PJ showed almost the same pressure distribution. In the cases of PJ with CH₄ fuel, the wall-pressure rise for the O₂ PJ was larger than that for the N₂ PJ, and for the O₂ PJ, the pressure rise started upstream of the PJ. Thus, the combustion by the O₂ PJ was stronger than that by the N₂ PJ, contrary to what was shown directly. This apparent inconsistency was caused by the difference of products around the torches and of the emission intensity of the torches. Shuzenji and Tachibana¹² spectroscopically measured the O₂ and N₂ PJ torches with CH₄ fuel injection. For the N₂ PJ, they found that there was a much stronger emission from CN radicals around the wavelength of 350–450 nm than from the N atoms. For the O₂ PJ, on the other hand, additional emission bands were weaker than those of the O atoms.

Discussion

Figures 8a and 8b show the remarkable effectiveness of the O₂ PJ for ignition and combustion of CH₄ fuel. The same tendency was also shown in the experimental result of Shuzenji and Tachibana¹²

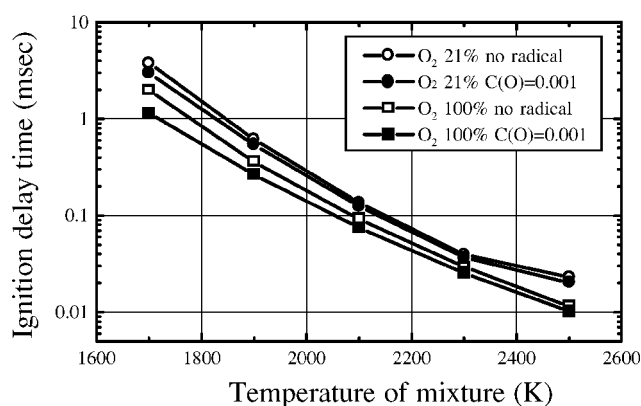


Fig. 12 Effects of radical addition on ignition delay time of CH₄/O₂/N₂ mixtures.

who suggested that the existence of oxygen radicals was the reason for the superiority. Figure 12 shows the calculated ignition delay time for the CH₄/air mixture with and without radical addition. In the figure, the O₂ mole fraction in the oxidizer is also a parameter to consider in a situation of high O₂ concentration in the collision of the O₂ PJ and the CH₄ jet. The O₂ fraction of 21% means that the oxidizer is air. It can be concluded from the figure that the increase in the O₂ mole fraction and the addition of O radicals to the mixture resulted in only a slight decrease of the ignition delay time of the CH₄/air mixture. Moreover, calculations of ignition delay time showed that the equivalence ratio of the mixture also had a weak effect on the ignition delay and that the most effective radicals in reducing the ignition delay of the CH₄/O₂/N₂ mixture were H radicals.¹³ Therefore, the superiority of the O₂ PJ to other PJs cannot be explained as being due to simple ignition phenomena with the addition of radicals. This tendency was also applicable to H₂ fuel. The most effective feedstock was the H₂/N₂ mixture in the ignition test of the H₂ fuel^{5,13}; on the other hand, the most effective radical for reducing the ignition delay of the H₂/air mixture was O radicals in

0-D analysis^{4,15}. The reason for the superiority of the H₂/N₂ PJ over other PJs for the H₂ fuel was considered an effect of combustion of the H₂ included in the PJ in the airflow after injection. On the other hand, in the case of the O₂ PJ to the CH₄ fuel, such a combustion effect did not exist; therefore, there was a different mechanism of the superiority of the O₂ PJ over other PJs for the CH₄ fuel from that of the H₂/N₂ PJ over other PJs for the H₂ fuel. The process of flame spread after the local ignition must be important.

Conclusions

1) Ignition and combustion of CH₄ and H₂ fuels occurred more easily for fuel injection upstream of the PJ than for injection downstream of the PJ. The PJ played the role of a flame-holder as well as of an igniter in the case of upstream injection.

2) The minimum P_{IN} required for ignition and the amount of combustion depended on the distance between the PJ and the fuel jet in the case of the upstream fuel injection. This result suggested that mixing of the fuel jet in the supersonic flow before it reached the PJ was an important factor in determining the amount of combustion.

3) The O₂ PJ showed remarkable superiority over other PJs for ignition and combustion of CH₄ fuel injected upstream of the PJ. This result cannot be explained as being due to simple ignition phenomena with addition of radicals.

4) The difference among PJs in the effectiveness for ignition and combustion of H₂ fuel in a supersonic flow was not so great, although weak dependence on feedstocks (the order was H₂/N₂, N₂, O₂) was seen in the case of downstream fuel injection.

Acknowledgment

This study was supported by Industrial Technology Research Grant 01B68004c from the New Energy and Industrial Technology Development Organization of Japan.

References

¹Kimura, I., Aoki, H., and Kato, M., "The Use of a Plasma Jet for Flame Stabilization and Promotion of Combustion in Supersonic Air Flows," *Combustion and Flame*, Vol. 42, 1981, pp. 297–305.

²Northam, G. B., McClinton, C. R., Wagner, T. C., and O'Brien, W. F.,

"Development and Evaluation of a Plasma Jet Flameholder for Scramjets," AIAA Paper 84-1408, 1984.

³Masuya, G., Kudou, K., Murakami, A., Komuro, T., Tani, K., Kanda, T., Wakamatsu, Y., Chinzei, N., Sayama, M., Ohwaki, K., and Kimura, I., "Some Governing Parameters of Plasma Torch Igniter/Flame-Holder in a Scramjet Combustor," *Journal of Propulsion and Power*, Vol. 9, No. 2, 1993, pp. 176–181.

⁴Takita, K., Uemoto, T., Sato, T., Ju, Y., Masuya, G., and Ohwaki, K., "Ignition Characteristics of Plasma Torch for Hydrogen Jet in an Airstream," *Journal of Propulsion and Power*, Vol. 16, No. 2, 2000, pp. 227–233.

⁵Masuya, G., Takita, K., Takahashi, K., Takatori, F., and Ohzeki, H., "Effects of Airstream Mach Number on H₂/N₂ Plasma Igniter," *Journal of Propulsion and Power*, Vol. 18, No. 3, 2002, pp. 679–685.

⁶Takita, K., "Ignition and Flame-Holding by Oxygen, Nitrogen and Argon Plasma Torches in Supersonic Airflow," *Combustion and Flame*, Vol. 128, No. 3, 2002, pp. 301–313.

⁷Takita, K., "Ignition by H₂/N₂ Plasma Torch in Supersonic Airflow," *Combustion Science and Technology*, Vol. 175, No. 4, 2003, pp. 743–758.

⁸Waltrup, P. J., "Upper Bounds on the Flight Speed of Hydrocarbon-Fueled Scramjet-Powered Vehicles," *Journal of Propulsion and Power*, Vol. 17, No. 6, 2001, pp. 1199–1204.

⁹Jacobsen, L. S., Gallimore, S. D., Schetz, J. A., O'Brien, W. F., and Goss, L. P., "Integration of an Aeroramp Injector/Plasma-Igniter for Hydrocarbon Scramjets," *Journal of Propulsion and Power*, Vol. 19, No. 2, 2003, pp. 170–182.

¹⁰Taguchi, H., Tomioka, S., Nagata, H., Takahashi, S., Ujii, Y., and Kono, M., "A Study on Supersonic Combustion Using Methane-Hydrogen Mixture Fuel," *Journal of the Japan Society of Aeronautical and Space Sciences*, Vol. 42, 1994, pp. 224–231 (in Japanese).

¹¹Ju, Y., and Niioka, T., "Ignition Simulation of Methane/Hydrogen Mixtures in a Supersonic Mixing Layer," *Combustion and Flame*, Vol. 102, 1995, pp. 462–470.

¹²Shuzenji, K., and Tachibana, T., "Superiority of Oxygen as Feedstock for a Plasma Jet Igniter in Supersonic Methane Air Streams," *Proceedings of the Combustion Institute*, Vol. 29, 2002, pp. 875–881.

¹³Takita, K., Moriwaki, A., Kitagawa, T., and Masuya, G., "Ignition of H₂ and CH₄ in High Temperature Airflow by Plasma Torch," *Combustion and Flame*, Vol. 132, No. 4, 2003, pp. 679–689.

¹⁴Masuya, G., Choi, B., Ichikawa, N., and Takita, K., "Mixing and Combustion of Fuel Jet in Pseudo-Shock Waves," AIAA Paper 2002-0809, Jan. 2002.

¹⁵Mitani, T., "Ignition Problems in Scramjet Testing," *Combustion and Flame*, Vol. 101, 1995, pp. 347–359.